



NJC

Visible light-induced photocatalytic activity of modified titanium (IV) oxide with zero-valent bismuth clusters

Journal:	<i>New Journal of Chemistry</i>
Manuscript ID:	NJ-ART-11-2014-001979.R1
Article Type:	Paper
Date Submitted by the Author:	14-Jan-2015
Complete List of Authors:	Remita, Hynd; LCP-CNRS, Laboratoire de Chimie Physique Kouamé, Natalie A.; Université Paris-Sud, Laboratoire de Chimie Physique Ouafa, TAHIRI ALAOUI; Université My Ismail, Morocco, Département de Chimie, Faculté des Sciences et Techniques Herissan, Alexandre; Université Paris-Sud, Laboratoire de Chimie Physique Larios, Eduardo; University of Texas at San Antonio, Department of Physics and Astronomy Colbeau, C; Université Paris-Sud, Laboratoire de Chimie Physique Jose - Yacaman, Miguel; university of Texas San Antonio, Physics Etcheberry, Arnaud; Université de Versailles Saint Querntin en Yvelines, Institut Lavoisier de Versailles

Visible light-induced photocatalytic activity of modified titanium (IV) oxide with zero-valent bismuth clusters

Natalie A Kouamé¹, Ouafa Tahiri Alaoui², Alexandre Herissan¹, Eduardo Larios^{3,4}, Miguel José-Yacaman³, Arnaud Etcheberry⁵, Christophe Colbeau-Justin¹ and Hynd Remita^{1,6}

¹ Laboratoire de Chimie Physique, UMR 8000-CNRS, Bât. 349, Université Paris-Sud, 91405 Orsay, France

² Département de Chimie, Faculté des Sciences et Techniques, Université My Ismail, Errachidia, Morocco

³ Department of Physics & Astronomy, The University of Texas at San Antonio, One UTSA Circle, San Antonio, TX 78249, USA

⁴ Departamento de Ingeniería Química y Metalurgia, Universidad de Sonora, 83000 Hermosillo, Sonora, Mexico

⁵ Institut Lavoisier de Versailles, CNRS UMR 8180, 45 Avenue des Etats Unis, 78035 Versailles, France

⁶ CNRS, Laboratoire de Chimie Physique, UMR 8000, 91405 Orsay, France.

E-mail address: hynd.remita@u-psud.fr. Tel: +33 1 69 15 72 58

Abstract. The important challenge in photocatalysis is to find efficient and stable photocatalysts under visible light. Small Bi zero-valence clusters were synthesized on TiO₂-P25 by radiolysis. Photocatalytic tests were conducted under UV, visible and solar light with rhodamine B and phenol taken as model pollutant. Surface modification of TiO₂ with zero valence Bi nanoclusters induces a high photocatalytic activity under visible light. Very small amount of Bi (0.5% wt.) can activate titania for photocatalytic applications under visible light. Time resolved microwave conductivity measurements indicate that under visible irradiation Bi nanoclusters inject electrons in the conduction band of TiO₂. These photocatalysts are very stable with cycling.

Keywords Titanium Dioxide, Zero Valent Bismuth Clusters, Photocatalysis, Water Treatment.

1. Introduction

TiO₂ is a very efficient photocatalyst due to its strong oxidation capacity, high photochemical and biological stability and low cost. TiO₂-based photocatalysts have attracted wide attention since the discovery of photoinduced decomposition of water on a TiO₂ electrode [1].

The limitation in TiO₂ application, results from low quantum yield because of the fast charge carriers (e^-/h^+) recombination and the necessity to use UV irradiation. Indeed, TiO₂ absorbs only 3-4 % of the solar light impinging on the Earth's surface as it can be excited only under UV irradiation with wavelengths shorter than 400 nm. Doping TiO₂ with N, C or S has been used to extent its activity towards the visible [2,3].

Doping TiO₂ with Rh³⁺ or Bi³⁺ ions also induced a photocatalytic activity under visible light [4-6]. Surface modification with noble metal ions, such as platinum, palladium, silver and gold or metal clusters and nanoparticles (NPs) can result in enhancements of the photo-conversion quantum yield and may allow the extension of the light absorption of wide band-gap semiconductors to the visible light [7-10]. In particular, plasmonic photocatalysts have appeared as a very promising way to enhance the activity of TiO₂ in the visible [11-15]. Noble metal-loaded titania photoreaction systems seem advantageous compared with other photosensitization systems using for example dye molecules, since noble metal deposits are relatively stable. Although if modification of titania with gold or silver nanoparticles results in photocatalytic activity under visible light, the development of cheap and efficient TiO₂-based photocatalysts without noble metals is still a challenge. Very few articles report on higher photocatalytic activity of TiO₂ under visible light obtained by its surface modification with non-noble metals, and in general the photocatalysts are not stable with cycling.

In this study, we investigated the modification of TiO₂ with Bi zero-valent nanoclusters for application in photocatalysis.

Bismuth is a cheap, abundant and non-toxic semi-metal. It exhibits interesting size-dependent electrical properties. Zero-valent bismuth (ZV-Bi) is a very attractive material for the study of quantum size effects due to its semi-metal electronic band structure, associated with a small overlap between the valence and the conduction band [16]. When zero-valence bismuth (ZV-Bi) nanoparticles (NPs) are smaller than 40 nm, a semi-metal to semi-conductor transition takes place [17]. The quantum confinement effects make bismuth a potential valuable material for thermoelectric, magnetoresistance [18], optical, and electro-optical devices applications [19]. Recently, semi-metal to semi-conductor phase transition induced by quantum confinement, has been measured for ZV-Bi NPs [20]. Indirect and direct energy gaps were found in the near-infrared range (1400-1600 nm) for ZV-Bi NPs of around 3.3 nm [20]. Calculations have shown that surface plasmon resonance of Bi nanoparticles can be tuned from the near-ultraviolet to the near-infrared range by changing the size and shape of bismuth nanoparticles and the dielectric constant of the environment [21,22].

Here we involve modification of TiO₂ with Bi zero-valent nanoclusters obtained by radiolytic reduction of Bi³⁺ on titania. Though Bi³⁺ doping is already reported, to our knowledge, it is the first time that Bi zero valent-clusters are used for surface modification of TiO₂. This surface modification leads to efficient photocatalytic activity under visible light and the photocatalysts are very stable with cycling.

2. Experimental details

2.1. Materials

Bismuth (III) chloride BiCl₃ (of 98% purity), and 2-propanol (99.9% purity) were obtained from Sigma Aldrich and used as received. N₂ gas (purity >99.995%) was purchased from Air Liquide. TiO₂ P25 was obtained from Evonik (80:20% anatase:rutile phase mixture with a surface area of 55 ± 15 m².g⁻¹). Phenol (of 99.5% purity), and rhodamine B (of 97% purity), were respectively purchased from Fluka and Sigma-Aldrich. Deionized water (Milli Q with 18.6 M U) was used all through our experiments.

2.2. Sample preparation

Bismuth nanoclusters were synthesized on TiO₂ by radiolytic reduction of Bi³⁺ on TiO₂ (x=0.1; 0.3; 0.5; 1 and 2 wt. % of Bi on TiO₂, the obtained photocatalysts were respectively named 0.1-Bi/TiO₂, 0.3-Bi/TiO₂, 0.5-Bi/TiO₂, 1-Bi/TiO₂, and 2-Bi/TiO₂). An appropriate mass (depending on the loading) of TiO₂ (P25 from Evonik) was put in suspension in an aqueous solution containing 10⁻³ M BiCl₃ and 0.1 M 2-propanol (to scavenge OH[•] radicals induced by radiolysis and to convert them into alcoholic reducing radicals).[23, 24] The suspension was first dispersed under stirring in the dark for 1 hour and sonicated for 5 minutes, degassed with nitrogen and then irradiated (under stirring) with a ⁶⁰Co panoramic gamma source (dose rate = 3 kGy h⁻¹, dose = 6 kGy). The bismuth ions were reduced by the solvated electrons and the alcohol radicals induced by solvent radiolysis.

2.3. Characterization of Modified TiO₂.

The samples were characterized by scanning transmission electron microscopy (STEM) using a JEOL ARM (200F): 200 kV FEGSTEM/TEM equipped with a CEOS Cs corrector on the illumination system. The probe current used for acquiring the high-angle annular dark field (HAADF)- and the bright field (BF)-STEM images was 9 C (23.2 pA); the aperture size of the

condenser lens was 40 mm. HAADF-STEM images were acquired with a camera length of 8 cm/6 cm and the collection angle of 68–280 mrad/90–270 mrad. The BF-STEM images were obtained using a 3 mm/1 mm aperture and a collection angle of 17 mrad/5.6 mrad (camera length in this case was 8 cm). The HAADF as well as the BF images were acquired using a digiscan camera. EDS measurements for line scan profiles as well as chemical maps for various elements were obtained with a solid state detector and software for two dimensional mapping from EDAX.

The diffusion reflectance spectra (DRS) of the modified TiO₂ samples were obtained using a Cary 5E spectrophotometer equipped with a Cary 4/5 diffuse reflection sphere. The baseline was recorded using a poly(tetrafluoroethylene) reference.

The X-ray photoelectron spectroscopy (XPS) analysis was performed on In foils. Sample drops were deposited on the foils and dried under N₂ flow. The XPS analyzer was a Thermo Electron ESCALAB 220i-XL. Either a non-monochromatic or a mono-chromatic X-ray Al K α line was used for excitation. The photo-electrons were detected perpendicularly to the support. A constant analyzer energy mode was used with a pass energy of 20 eV.

The charge-carrier lifetimes in TiO₂ after UV and visible illumination were determined by microwave absorption experiments using the Time Resolved Microwave Conductivity method (TRMC) [25, 26]. The TRMC technique is based on the measurement of the change of the microwave power reflected by a sample, $\Delta P(t)$, induced by its laser pulsed illumination. The relative difference $\Delta P(t)/P$ can be correlated, for small perturbations of conductivity, to the difference of the conductivity $\Delta\sigma(t)$ considering the following equation:

$$\frac{\Delta P(t)}{P} = A\Delta\sigma(t) = Ae \sum_i \Delta n_i(t)\mu_i$$

where $\Delta n_i(t)$ is the number of excess charge-carriers i at time t and μ_i their mobility. The sensitivity factor A is independent of time, but depends on different factors such as the microwave frequency or the dielectric constant. Considering that the trapped species have a small mobility which can be neglected, Δn_i is reduced to mobile electrons in the conduction band and holes in the valence band. And in the specific case of TiO₂, the TRMC signal can be attributed to electrons because their mobility is much larger than that of the holes [27].

The incident microwaves were generated by a Gunn diode of the K α band at 30 GHz. Pulsed light source was an OPO laser (EKSPLA, NT342B) tunable from 225 to 2000 nm. It delivers 8 ns fwmh pulses with a frequency of 10 Hz. The light energy densities received by the sample were respectively 1.2, 3.4, 7.0, 4.5 and 4.2 mJ·cm⁻² at 355, 410, 450, 500 and 510 nm.

2.4. Photocatalytic tests

The modified TiO₂ photocatalysts were separated by centrifugation and they were dried at 60°C. In this study, we used three reactors. The first reactor was illuminated by visible light with an Oriel 300 W xenon lamp, equipped with an optical filter cutting-off wavelengths shorter than 450 nm. The volumes of the solutions used in this reactor were 4 mL. The second reactor (Heraeus UV-RS1) was illuminated with a lamp simulating the solar light (xenon TXE 150 W). Figure S1 shows the emission spectrum of this lamp. The volumes of the solutions used for Heraeus UV-RS1 were 300 mL.

A fixed volume (from 600 µL to few mL depending on the reactor) of the irradiated suspension was sampled from the reactor at different time points and was centrifuged to separate the catalyst to get transparent solution.

The photocatalytic activity of x-Bi/TiO₂ powders was estimated by measuring the decomposition rate of phenol (initial concentration 3.7×10^{-3} mol.L⁻¹) and rhodamine B (initial concentration 10^{-4} mol.L⁻¹) in aqueous solution. The concentrations of phenol was determined using HPLC Agilent 1260 infinity quaternary LC equipped with a UV-detector (set at 260 nm for phenol). The column was an Adsorbosphere C18 reverse phase (5µm, l= 150 mm, ID: 4.6 mm, Alltech) combined with an All-Guard cartridge systemTM (7.5x 4.6 mm, Alltech).

To determine the concentration of rhodamine B, we used a HP Agilent diode array 8453 UV-visible spectrophotometer.

The Total Organic Carbon (TOC) was measured by using a Shimadzu TOC-LCSH. TOC was measured by IR after complete oxidation by catalytic combustion at 680 °C on exclusive platinum catalyst, the inorganic carbon being removed by a previous acidification and air purging.

The photocatalytic experiments were conducted with 1g.L⁻¹ of photocatalyst.

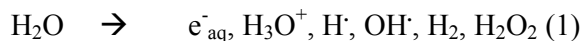
The stability of the modified photocatalysts with recycling was studied in the Heraeus reactor. The degradation of phenol and its mineralisation were followed by HPLC and TOC. After a complete degradation reaction, phenol was added for a new cycle of degradation. This test was realized three times.

Other photocatalytic tests have been conducted under real solar irradiation: the experiments have been realized in Morocco with a reactor directly exposed to solar light using 500 mg.L⁻¹ of the photocatalyst. The volumes of the solutions used were 500 mL.

3. Results and discussion

3.1. Radiolytic synthesis

Aqueous solutions containing BiCl₃ and TiO₂ were exposed to γ -rays. The primary effects of the interaction of high-energy radiation such as particle beams, X-rays or gamma photons with a solution of ions are the excitation and the ionization of the solvent.²³ For example, in aqueous solutions according to equation (1):



During the irradiation of deoxygenated water, hydroxyl radicals (HO \cdot), which are very strong oxidative species, are also formed. To avoid competitive oxidation reactions which may limit or even prevent bismuth reduction, 2-propanol (0.1M) was added in solution prior to irradiation to scavenge hydroxyl radicals leading to reducing alcohol radicals (CH₃)₂C \cdot OH. Bi ions are reduced by solvated electrons and alcohol radicals. Radiolysis is a powerful method to synthesize nanoparticles of controlled size and shape in solution and in heterogeneous media.[23, 24] Solvent radiolysis induces formation of solvated electrons and radicals which reduce the metal ions homogeneously in the medium leading to a homogeneous nucleation. Small and relatively monodisperse nanoparticles can therefore be obtained. Radiolysis presents the advantage of inducing a homogeneous nucleation and growth in the whole volume of the sample and has been successfully used in order to synthesize various noble (such as silver, gold and platinum) and non-noble (such as nickel and iron) metal nanoparticles in solutions or on supports.

3.2. Characterization of the materials.

The modified photocatalysts Bi/TiO₂ were very slightly grey. High-angle annular dark field (HAADF) and bright field (BF)-scanning transmission electron microscopy (STEM) images show homogeneous Bi nanoclusters homogeneously dispersed on TiO₂ (figure 1 and figure S2). Nanoclusters with mean sizes of 1.2 nm and 1 nm to subnanometer clusters were obtained respectively for the metal loadings 2 wt.% and 0.5 wt.%. The contrast of the images is roughly proportional to Z^2 where Z is the atomic number. Therefore due to the difference of the atomic number of Ti and Bi, the contrast is easy to see. The bright spots correspond therefore to Bi nanoclusters. Indeed, EDS analysis attest that the clusters deposited on TiO₂ are composed of Bi (figure 2).

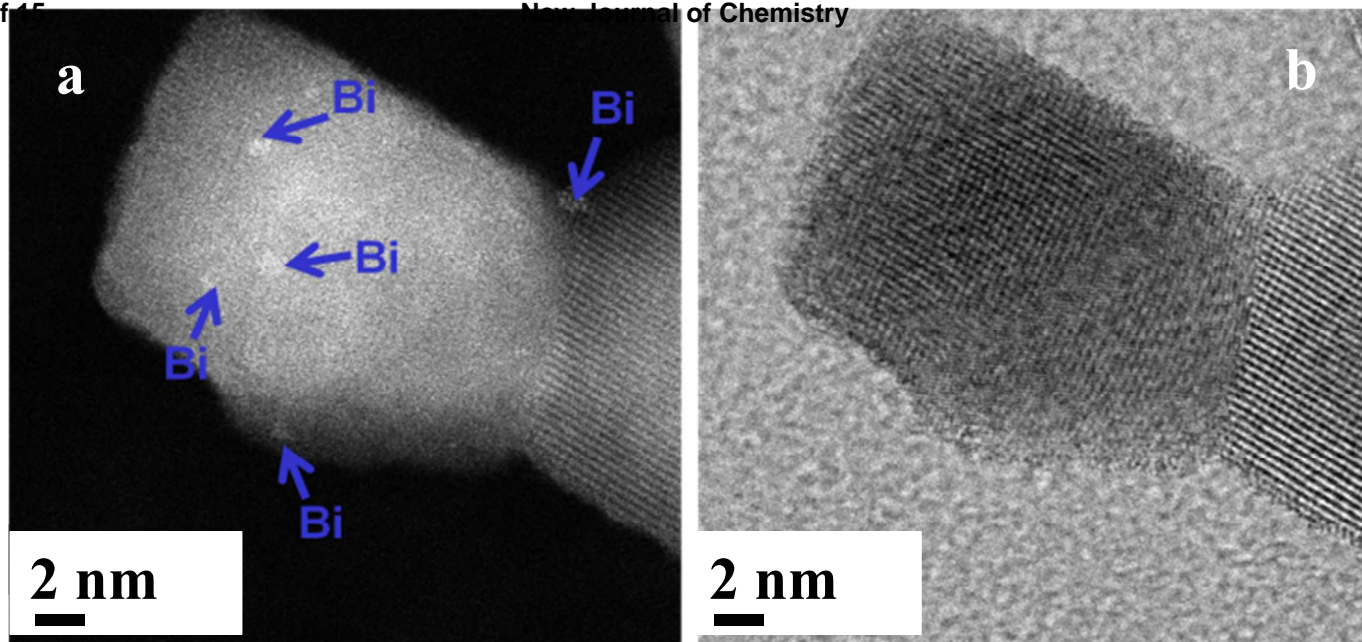


Figure 1. HAADF-STEM (a) and BF-STEM (b) images of 0.5-Bi/TiO₂.

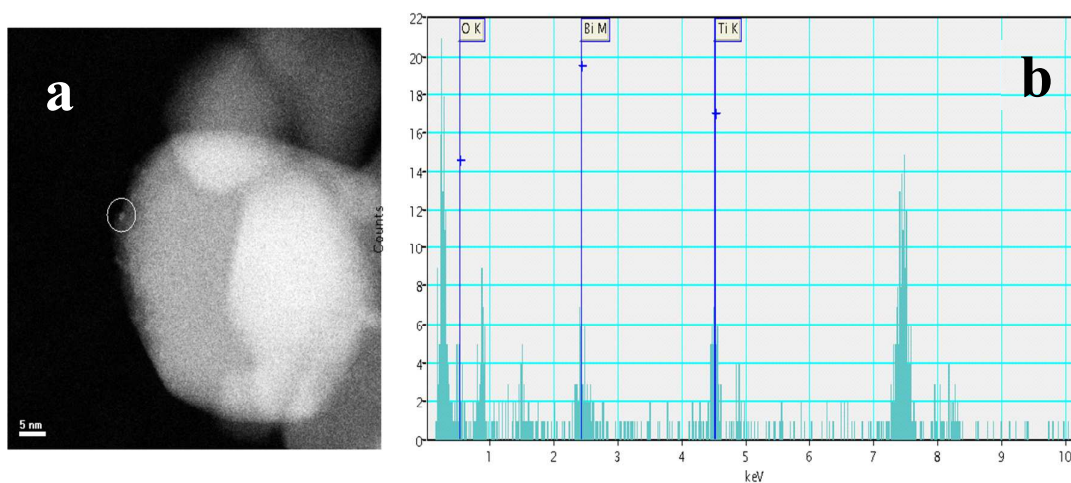


Figure 2. HAADF images (a) and EDS analysis of 2-Bi/TiO₂ (b).

The XPS survey of the sample 1-Bi/TiO₂ is shown in figure S3. The Bi 4f peak shape has a split doublet that correlates with Bi 4f_{7/2} and Bi 4f_{5/2} (figure 3). The split Bi 4f_{5/2} and Bi 4f_{7/2} peaks of the samples can be deconvoluted into four peaks. The two main peaks at 162.0 and 156.7 eV are in good agreement with the values reported in the literature for the Bi 4f_{5/2} and 4f_{7/2} binding energies of metallic bismuth, which are 162.4 and 157.1 eV, respectively. The other two weak peaks shifting towards higher binding energies indicates the existence of a very small amount of bismuth oxide (Bi³⁺: 4f_{7/2}, 159.3 eV; 4f_{5/2}, 164.7 eV) or more likely, due to Bi in strong interaction with the oxygen atoms of TiO₂.

These characterization results show that radiolytic reduction of Bi^{3+} on TiO_2 led to subnanometer zero-valent clusters quite homogeneous in size. It has to be noticed, that there are the smallest ZV-Bi nanoclusters described in the literature.

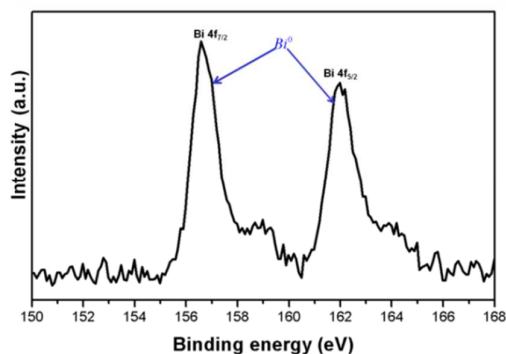


Figure 3. Bi 4f_{7/2} (162.0 eV) and Bi 4f_{5/2} (156.7 eV) XPS spectra of the sample 1-Bi/TiO₂.

The optical properties of the modified TiO₂ have been studied by Diffuse Reflectance Spectroscopy. Figure 4 shows the spectra of pure and modified TiO₂. The DRS of the modified samples show a slight shift in the band-gap transition to longer wavelengths for all kinds of surface-modified photocatalysts. This effect was previously observed with Pt- and Ag- modified TiO₂ [7,13]. This can be attributed to a stronger stabilization of the conduction band of TiO₂ by the interaction with the Bi nanoclusters compared to the stabilization of the valence band. The absorbance in the visible region is slightly higher for the modified titania than for pure TiO₂.

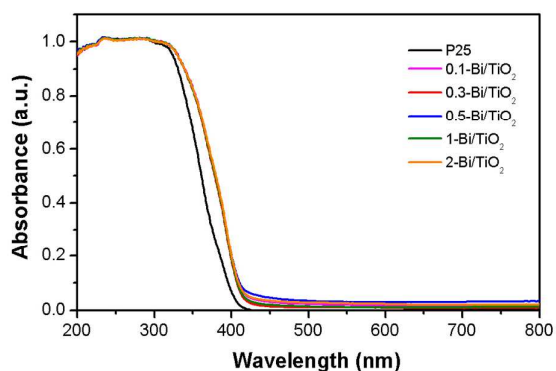


Figure 4. Diffuse reflectance spectra of x-Bi/TiO₂ and bare P25 TiO₂.

3.3. Photocatalytic tests.

TiO₂ Evonik P25 (mixture anatase –rutile 80%-20%) is not photoactive under visible light because the illumination energy is below the bandgap. We studied the degradation of phenol and rhodamine B (taken as model pollutants) under visible and solar light. The degradation of phenol was studied by HPLC and the degradation of rhodamine B by UV-Visible spectroscopy. Experiments with the total organic carbon (TOC) technique were conducted to study the mineralization of phenol at different irradiation times. Adsorption tests in the dark showed that phenol and rhodamine do not adsorb on the surface of the Bi modified TiO₂ (figure S4).

The total photodegradation of the model pollutants under visible light is efficient with Bi-modified P25, the faster degradation was obtained with 0.5-Bi/TiO₂: 100% of RhB and 30 % of the phenol were degraded after 230 minutes irradiation under visible light ($\lambda \geq 450$ nm) (figure 5). The apparent rate constants of the first-order kinetic of phenol photodegradation for the bare- and modified TiO₂ are given in Table S1. Modification with 0.5 % wt. amount of Bi leads to a better enhancement of the photocatalytic properties. The sizes of the Bi clusters increase very slightly with loading. This highest activity obtained with 0.5-Bi/TiO₂ may be due to the best surface coverage or interaction with P25 TiO₂ at this loading. Higher density of Bi nanoclusters on TiO₂ surface could act as recombination centers decreasing the photocatalytic activity.

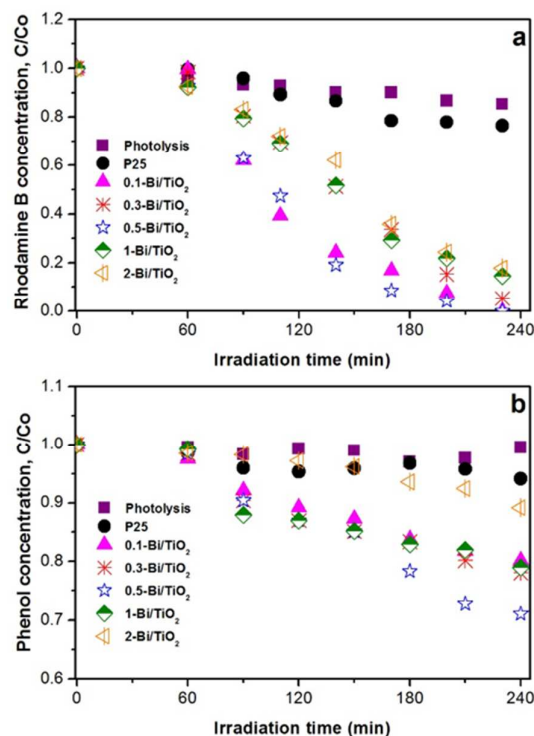


Figure 5. Photodegradation of (a) Rhodamine B (initial concentration 10^{-4} mol.L $^{-1}$) and (b) Phenol (initial concentration 3.7×10^{-3} mol.L $^{-1}$) with x-Bi/TiO $_2$ (1 g.L $^{-1}$) under visible illumination ($\lambda > 450$ nm: A Xenon lamp was used with a filter cutting the wavelengths below 450 nm).

The photocatalytic activity of the Bi-modified TiO $_2$ photocatalysts was compared to that of Ag-modified TiO $_2$ prepared by radiolysis.¹³ Interestingly, under visible light, Bi-TiO $_2$ photocatalysts show a higher photocatalytic activity than plasmonic Ag-modified TiO $_2$: 30% of phenol is degraded with 0.5Bi-TiO $_2$ after 240 min irradiation as compared to only 18% with Ag-TiO $_2$.

The experiments under real solar light show also a good photocatalytic activity of the Bi-modified TiO $_2$ and the best degradation kinetics of the model pollutants were obtained also with the sample 0.5-Bi/TiO $_2$. These results are shown in figure S5.

Tests have been conducted to study the stability of the photocatalysts. Figure 6 shows that the photocatalysts are highly stable: After different cycles, the photocatalytic activity does not decrease. The stability of these photocatalysts is an important issue for practical applications.

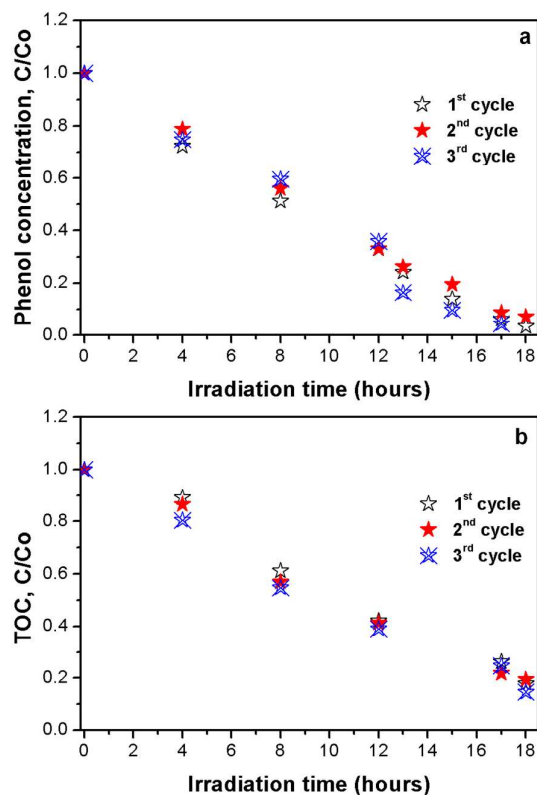


Figure 6. Evolution of the photocatalytic activity on aging of 0.5-Bi/TiO₂ (1 g.L⁻¹) for phenol degradation and mineralization (initial concentration 3.7×10⁻³ mol.L⁻¹) with a reactor simulating solar light (the spectrum of the lamp is given in figure S1): (a) Decrease of phenol concentration based on HPLC measurements, and (b) the disappearance of Total Organic Carbon.

3.4. Study of Charge carrier dynamics

Time Resolved Microwave Conductivity is a very useful technique to study the charge carrier dynamics, which is a key factor in photocatalysis. Modified TiO₂ was studied under UV and visible irradiation at different wavelengths (excitation with an OPO laser of tunable wavelengths).

The intensity of the TRMC signals of the modified TiO₂ under UV illumination is higher compared to the one obtained with bare TiO₂ (figure 7(a) and table S2) indicating that more electrons are induced in the conduction band of Bi-modified TiO₂. This result indicates that Bi clusters inject electrons in the conduction band of TiO₂. On the other hand, the decays of TRMC signals obtained with modified and non-modified TiO₂ are very similar indicating that the Bi nanoclusters do not have an influence on charge carrier recombination or trapping. Anyway, under UV light modification of P25-TiO₂ with Bi nanoclusters does not significantly increase its photocatalytic activity.

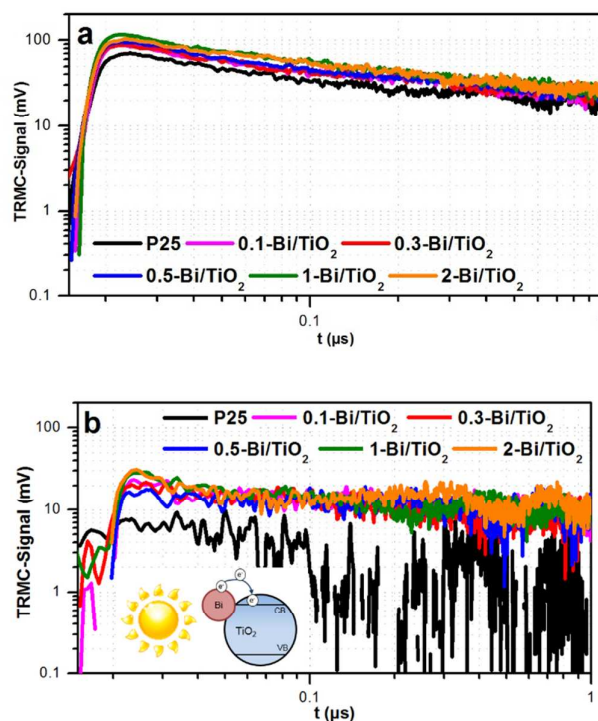


Figure 7. TRMC signal of bare and Bi-modified samples obtained by irradiation at 355 nm (a) and 450 nm (b). The excitation densities were respectively 1.2 and 7 $\text{mJ}\cdot\text{cm}^{-2}$. Inset: A scheme showing electron injection from Bi nanoclusters in the conduction band of TiO_2 under visible light excitation.

The signals obtained under visible (450 nm) irradiation are very different for bare and modified TiO_2 as shown in figure 7(b): The surface modification with Bi clusters induces a TRMC signal after excitation in the visible, which is not the case for pure TiO_2 . This proves that electrons are produced under visible illumination in the conduction band of Bi-modified P25. These electrons are due to the electrons injected from the excited Bi nanoclusters in the conduction band of TiO_2 . This charge carrier generation can explain the photocatalytic activity for phenol and RhB degradation under visible light. This electron injection under visible light has been also suggested in the case of plasmonic photocatalysts under visible irradiation [11, 13, 15]. In our case, the photocatalysts cannot be considered as plasmonic ones as the Bi clusters are too small. Under excitation at 500 nm (figure S6), there is still a weak TRMC signal, indicating that electrons are injected from Bi nanoclusters to the conduction band of TiO_2 , while no more signal is obtained at larger excitation wavelengths, as shown for example in Fig. S6c, under excitation at 550 nm.

In the case of surface modification with Bi clusters, the excitation under visible light induces ejection of electron from Bi clusters to the conduction band of TiO_2 , which is responsible of the photocatalytic activity under visible light. It has been reported that doping TiO_2 with Bi^{3+} leads to extension of absorption of TiO_2 into the visible light region. Doping with Bi^{3+} induces new intermediate energy states and intrinsically narrows the band-gap of TiO_2 .²⁸⁻³⁰ In this case, the mechanism responsible of the visible light activity is different from the one observed in the present work with surface modification with Bi nanoclusters.

Further experiments will be conducted to optimize the size of Bi clusters on TiO_2 in the aim to improve the photocatalytic activity of the modified titania for applications under solar light. As the photoactivity of modified TiO_2 depends on its properties, modification of different titania, including pure anatase will be also considered.

4. Conclusion

Zero-valent Bi nanoclusters homogeneous in size (1.3 nm) were synthesized on P25 TiO_2 by radiolysis. Photocatalytic tests have been conducted with rhodamine B and phenol as model

pollutants. Titania surface modification with Bi nanoclusters enables the increase of the photocatalytic activity under visible irradiation and solar light. The TRMC signals of the Bi-modified TiO₂ under UV and visible illumination ($\lambda \leq 450$ nm) indicate that Bi nanoclusters inject electrons in the conduction band of TiO₂. This injection of electrons in the conduction band of TiO₂ under visible light is responsible of the photocatalytic activity of Bi-modified TiO₂.

The highest photocatalytic activity is obtained with P25 modified with Bi at mass loading of 0.5 wt.%. These photocatalysts show higher photocatalytic activity under visible light than plasmonic Ag-modified TiO₂ and they are very stable with cycling. Considering that bismuth is very abundant and non-toxic, surface modification of TiO₂ with Bi clusters can lead to cheap, eco-friendly and efficient photocatalysts under solar light. These nanomaterials can also find applications in photovoltaics and solar cells.

Acknowledgments

The authors acknowledge C’Nano Ile de France and the RTRA - Triangle de la Physique for the financial support for TRMC set-up and panoramic gamma source. The authors would also like to acknowledge the Welch Foundation Agency Project # AX-1615, the NSF for grants PREM 0934218 and Grant 1103730 “Alloys at the Nanoscale; The Case of Nanoparticles Second Phase” and to the National Institute on Minority O.T.A. acknowledges the Agence Universitaire de la Francophonie (AUF) for financial support.

Associated content

Supporting Information

Additional HAADF images of Bi-modified TiO₂, spectrum of a reactor lamp, photocatalytic tests under solar light, and additional TRMC signal. This information is available free of charge via the Internet at <http://www.rsc.org>.

References

- [1] A. Fujishima and K. Honda, *Nature*, **1972**, *238*, 37-38.

- [2] R. Asahi, T. Morikawa, T. Ohwaki, K. Aoki and Y. Taga, *Science*, **2001**, *293*, 269-271.
- [3] S. Sakthivel and H. Kisch, *ChemPhysChem*, **2003**, *4*, 487-490.
- [4] S. Kitano, N. Murakami, T. Ohno, Y. Mitani, Y. Nosaka, H. Asakura, K. Teramura, T. Tanaka, H. Tada, K. Hashimoto and H. Kominami, *J. Phys. Chem. C*, **2013**, *117*, 11008-11016.
- [5] Z. Ximiao, L. Zhang, F. Jianzhang, S. Wu and W. C. Xu, *J. Mater. Res.*, **2013**, *28*, 1334-1342.
- [6] S. Murcia-Lopez, M. C. Hidalgo and J. A. Navio, *Appl. Catal. A-Gen.*, **2011**, *404*, 59-67
- [7] E. Kowalska, H. Remita, C. Colbeau-Justin, J. Hupka and J. Belloni, *J. Phys. Chem. C*, **2008**, *112*, 1124-1131.
- [8] P. V. Kamat, *J. Phys. Chem. B*, **2002**, *106*, 7729-7744.
- [9] P. V. Kamat, *J. Phys. Chem. Lett.*, **2012**, *3*, 663-672.
- [10] Z. Hai, N. E. Kolli, D. B. Uribe, P. Beaunier, M. Jose-Yacaman, A. Etcheberry, S. Sorgues, C. Colbeau-Justin, J. F. Chen and H. Remita, *J. Mater. Chem. A*, **2013**, *1*, 10829-10835.
- [11] S. Linic, P. Christocher and D. B. Ingram, *Nature Mater.*, **2011**, *10*, 911-921.
- [12] Y. Tian and T. Tatsuma, *J. Am. Chem. Soc.*, **2005**, *127*, 7632-7637.
- [13] E. Grabowska, A. Zaleska, S. Sorgues, M. Kunst, A. Etcheberry, C. Colbeau-Justin and H. Remita, *J. Phys. Chem. C*, **2013**, *117*, 1955-1962.
- [14] Y. Horiguchi, T. Kanda, K. Torigoe, H. Sakai and M. Abe, *Langmuir*, **2014** *30*, 922-928
- [15] S. W. Verbruggen, M. Keulemans, M. Filipousi, D. Flahaut, G. Van Tendeloo, S. Lacombe, J. A. Martens and S. Lenaerts, *Appl. Catal. B-Environ.* **2014**, *156-157*, 116-121.
- [16] M. H. Mikkela, M. Tchapyguine, S. Urpelainen, K. Jankala, O. Björneholm and M. Huttula, *J. Appl. Phys.*, **2012**, *112*, 084326.
- [17] Y. W. Wang, J. S. Kim, G. H. Kim and K. S. Kim, *Appl. Phys. Lett.*, **2006**, *88*, 143106-1-143106-3.
- [18] Z. Zhang, X. Sun, M. S. Dresselhaus, J. Y. Ying and J. Heremans, *Phys. Rev. B.*, **2000**, *61*, 4850-4861
- [19] T. W. Cornelius and M. E. Toimil-Morales *Nanowires* ed Praola Prete (Croatia) Intech **2010** pp 414-437.
- [20] D. Velasco-Arias, I. Zumeta-Dubé, D. Díaz, P. Santiago-Jacinto, V. F. Ruiz-Ruiz, S. E. Castillo-Blum and L. Rendón, *J. Phys. Chem. C*, **2012**, *116*, 14717-14727.
- [21] J. Toudert, R. Serna and M. Jiménez de Castro, *J. Phys. Chem. C*, **2012**, *116*, 20530-20539.

- [22] J. M. McMahon, G. C. Schatz and S. K. Gray, *Phys. Chem. Chem. Phys.*, **2013**, *15*, 5415–5423.
- [23] J. Belloni, M. Mostafavi, H. Remita, J. L. Marignier and M. O. Delcourt, *New J. Chem.*, **1998**, *22*, 1239-1255.
- [24] Z. Hai, N. EL Kolli, J. Chen, H. Remita, *New J. Chem.* **2014**, *38*, 5279 – 5286.
- [25] C. Colbeau-Justin, M. Kunst, and D. Huguenin, *J. Mater. Sci.*, **2003**, *38*, 2429-2437.
- [26] M. Kunst, F. Goubard, C. Colbeau-Justin and F. Wünsch, *Mater. Sci. Eng. C*, **2007**, *27*, 1061–1069.
- [27] S. J. Fonash *Solar Cell Device Physics* Academic Press (New York, London) **1981**.
- [28] A. Hamdi, A.M. Ferraria, A.M. Botelho do Rego, D.P. Ferreira, D.S. Conceição, L.F. Viera Ferreira, S. Bouattour, *J. Mol. Catal. A: Chem.* **2013**, *380*, 34-42.
- [29] H.S. Zuo, J. Sun, K.J. Deng, R. Su, F.Y. Wei, D.Y. Wang, *Chem. Eng. Technol.* **2007**, *30*, 577-582.
- [30] S. Sood, S. K. Mehta, A. Umar, S. K. Kansal, *New J. Chem.*, **2014**, *38*, 3127-3136.